Weierstraß-Institut
für Angewandte Analysis und Stochastik
Leibniz-Institut im Forschungsverbund Berlin e. V.

Preprint ISSN 2198-5855

Symmetry breaking and strong persistent plasma currents via resonant destabilization of atoms

Carsten Brée[1], Michael Hofmann[2], Ihar Babushkin[3], Ayhan Demircan[3], Uwe Morgner[3], Olga G. Kosareva[4], Andrei B. Savel'ev[4], Anton Husakou[5], Misha Ivanov[5]

submitted: September 5, 2017

[1] Weierstrass Institute
Mohrenstr. 39
10117 Berlin, Germany
E-Mail: carsten.bree@wias-berlin.de

[2] Virtimo AG
Münzstr. 5
10178 Berlin, Germay
E-Mail: michael.hofmann@virtimo.de

[3] Leibniz Universität Hannover
30167 Hannover, Germany
E-Mail: babushkin@iqo.uni-hannover.de
morgner@iqo.uni-hannover.de
demircan@iqo.uni-hannover.de

[4] Lomonosow State Unversity
Moskow, Russia
E-Mail: kosareva@physics.msu.ru
abst@physics.msu.ru

[5] Max Born Institute
12489 Berlin, Germany
E-Mail: gusakov@mbi-berlin.de
mikhail.ivanov@mbi-berlin.de

No. 2423

Berlin 2017

2010 *Mathematics Subject Classification.* 78A60, 35P25.

2010 *Physics and Astronomy Classification Scheme.* 32.80.Rm,42.65.Ky,42.50.Hz.

Key words and phrases. THz light generation, photoionization, multiphoton dynamics, Floquet theorem.

I.B., U.M., and M.I. gratefully acknowledge the support of the DFG QUTIF programme. A.B.S., O.G.K. acknowledge the support from Russian Science Foundation (Grant No. 16-42-01060). U.M. acknowledge the support of DFG (project MO 850-20/1). M.H. and C.B. acknowledge funding by DFG (grant BR 4654/1).

Edited by
Weierstraß-Institut für Angewandte Analysis und Stochastik (WIAS)
Leibniz-Institut im Forschungsverbund Berlin e. V.
Mohrenstraße 39
10117 Berlin
Germany

Fax: +49 30 20372-303
E-Mail: preprint@wias-berlin.de
World Wide Web: http://www.wias-berlin.de/

Symmetry breaking and strong persistent plasma currents via resonant destabilization of atoms

Carsten Brée, Michael Hofmann, Ihar Babushkin, Ayhan Demircan, Uwe Morgner, Olga G. Kosareva, Andrei B. Savel'ev, Anton Husakou, Misha Ivanov

Abstract

The ionization rate of an atom in a strong optical field can be resonantly enhanced by the presence of long-living atomic levels (so called Freeman resonances). This process is most prominent in the multiphoton ionization regime meaning that ionization event takes many optical cycles. Nevertheless, here we show that these resonances can lead to fast subcycle-scale plasma buildup at the resonant values of the intensity in the pump pulse. The fast buildup can break the cycle-to-cycle symmetry of the ionization process, resulting in generation of persistent macroscopic plasma currents which remain after the end of the pulse. This, in turn, gives rise to a broadband radiation of unusual spectral structure forming a comb from terahertz (THz) to visible. This radiation contains fingerprints of the attosecond electronic dynamics in Rydberg states during ionization.

Dynamics of atomic photoionization is central to many recent advances in optics and in physics in general, such as attosecond physics and attosecond metrology via high harmonic generation (HHG) which allowed generation of coherent radiation at frequencies up to many hundreds of eV, dramatically extending the range where coherent ultrashort pulses are available [1, 2]. Ionization-induced dynamics can also be used to generate frequencies in the opposite — low-frequency — range, namely in the terahertz (THz) [3, 4, 5, 6, 7]. Radiation at THz frequencies can be generated in filaments via wake fields (longitudinal plasma oscillations) [8] or via Cherenkov radiation [9]. However, a much more efficient mechanism is based on the fast step-like tunnel ionization process in strong fields, resulting in formation of persistent macroscopic currents [3, 4, 5, 6, 7, 10]. For this, one needs to have asymmetric incident waveforms (e.g. using two- or multi- color fields) [4, 5, 10, 11], so that the macroscopic currents created by the positive field half-cycles are not compensated by the currents created during the negative half-cycles. As a result, persistent current arises and does not disappear after the end of the pulse. The step-like nature of tunnel ionization is of critical importance for this method: in the deep multiphoton regime, as the sub-cycle steps in the ionization dynamics gradually disappear, the method appears to fail [12].

Here we use the so-called Freeman resonances, arising in the multiphoton regime [13], to create a new source of such asymmetry. Freeman resonances appear when the excited atomic states are Stark-shifted by the strong laser field in and out of n-photon resonances. In that case, the population transfer in the atom is dominated by two major competing mechanisms: resonantly enhanced ionization by direct electronic transitions from the ground state into the continuum, and population trapping in high-lying, laser-dressed and strongly distorted states [14]. The latter can be viewed as the extension of the Kramers-Henneberger concept [15, 16] to the Rydberg manifold [17, 18, 19].

In this letter we show that Freeman resonances produce radiation in a broad frequency range and point out that this radiation contains information about the ionization dynamics. Namely, we show that Freeman resonances are able to produce rather short spikes of ionization, with dynamics even on a

DOI 10.20347/WIAS.PREPRINT.2423 Berlin 2017

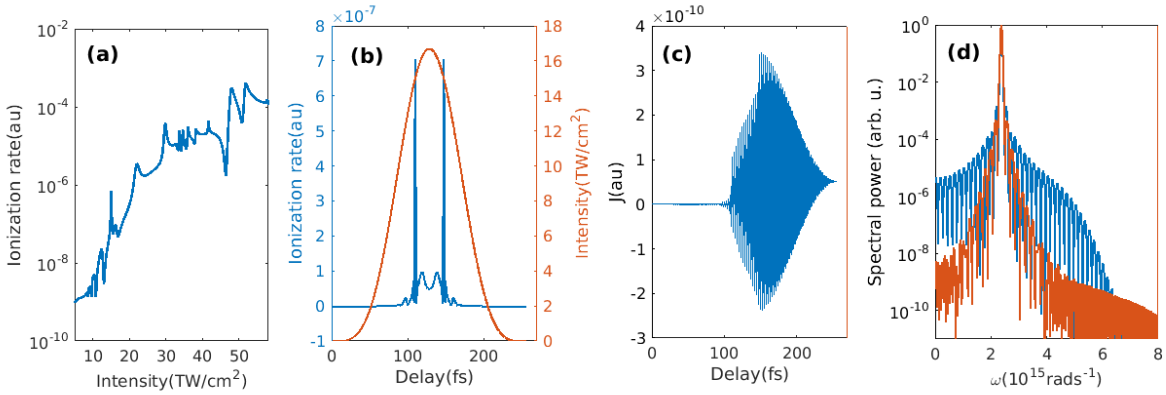

Figure 1: (a) Ionization rate in dependence of the pump intensity; Peaks in ionization rate are Freeman resonances. (b) Intensity (red) and the corresponding ionization rate (blue) generated by a long pulse of the form described in text, with the wavelength 800 nm, duration 240 fs and peak intensity 17 TW/cm^2. (c) Macroscopic free electron current; Persistent currents after the field passage are visible. (d) The spectrum of the corresponding radiation E_f given by Eq. (2) for the pulse in (b,c) (blue line) and in the case of the pulse with the same parameters by the intensity 23 TW/cm^2 (red line).

sub-cycle level. This sub-cycle dynamics breaks the symmetry of the ionization process, leading to the generation of a new comb-like structure in a broad frequency range from THz to visible. The comb-like structure is a result of interference from different ionization events. The same multi-event structure contains signatures of the electron dynamics “half-way” to the continuum, in particular, of “frustrated tunneling” [19].

First, we will develop an “adiabatic” approach to the problem, which allows to describe the underlying physics qualitatively. Next, we confirm our model with the direct solution of the time-dependent Schrödinger equation.

In the adiabatic regime, we consider the ionization dynamics in a long pulse with a slowly varying envelope. To develop the adiabatic approach, we first find the ionization rate using the non-Hermitian Floquet framework for monochromatic optical fields in the multiphoton regime [20, 21]. That is, we assume a strictly periodic field $E = E_0 \cos(\omega_0 t)$ with $\omega_0 = 0.057$ a.u. Then, we search for the Floquet resonances in the eigenvalue problem $(H - i\partial_t)\psi(x,t) = \epsilon_\alpha \psi(x,t)$ where H describes the system Hamiltonian, ϵ_α is the complex quasi-energy such that the Floquet eigenfunctions $\Psi = e^{-i\epsilon_\alpha}\psi$ are quasi-periodic in time: $\Psi(x, t+T) = e^{-\epsilon_\alpha T}\Psi(x,t)$, $T = 2\pi/\omega_0$. The ionization rate is determined by the inverse lifetime of the resonances $\Gamma_\alpha = -2\,\mathrm{Im}\,\epsilon_\alpha$ [22]. For simplicity, we consider here 1-dimensional evolution with the Hamiltonian

$$H = -\frac{1}{2}\partial_{xx} - \frac{1}{\sqrt{x^2+a^2}} - iA(x)\partial_x, \tag{1}$$

where $A(x)$ is the vector potential corresponding to the electric field $E(t)$ of the pump pulse. A soft-core potential with $a = \sqrt{2}$ was used, allowing to reproduce the ionization energy of atomic hydrogen ($I_p = 13.6$ eV) [21].

Separating the time scales of the slow envelope and the fast carrier oscillation allows us to apply the adiabatic theorem of quantum mechanics [23], which implies that at each instant of time, the atom remains in the Floquet resonance which is adiabatically connected to the ground state. Also, in this approximation, the population of intermediate levels is negligible and the ionization yield is completely determined by the imaginary part of the Floquet quasienergy. Numerically, the Floquet eigenproblem

was solved by discretizing it in a sufficiently large numerical box (we used 200 au), which supports the relevant resonant states.

Dependence of the ionization rate $\Gamma_0[I]$ of the grond-state resonance on the intensity I is shown in Fig. 1(a), exhibiting several narrow resonances. In Fig. 1(b) we show the pulse of the shape $E(t) = E_0 \sin(\omega_0 t) \sin(\pi t/T)^2$ with $T = 2\pi/\omega_0$ being the pulse duration and E_0 the peak field strength (red line in Fig. 1(b) shows the pulse envelope). The corresponding ionization rate is shown in Fig. 1(b) by a blue curve. One can see that when the intensity of the pulse, which changes in time, passes the resonant intensity (e.g. around 15 TW/cm^2), sharp spikes in the ionization rate take place, which correspond to the Freeman resonances. The corresponding plasma current is shown in Fig. 1(c) and is obtained from the Drude model without damping via $\partial_t J(t) = \rho(t)E(t)$, with a plasma density ρ governed by a rate equation $\partial_t \rho = \Gamma_\alpha[I(t)](\rho_0 - \rho)$. The current contains fast oscillations reflecting electron dynamics at the frequency ω_0, but the important point is that after the pulse the current does not return to zero as would have happened if the resonances were not present.

It is also known that the change of the macroscopic free current J due to ionization can produce radiation (Brunel harmonics) [24, 25, 5, 10, 26, 12]. More specifically, if we assume that plasma arises in a small spatial spot, the corresponding field at the observer point will be governed by the expression:

$$E_f(t) = g\frac{dJ(t)}{dt} = g\frac{d^2P(t)}{dt^2}, \tag{2}$$

where g is an constant depending on the observation point. We also introduced formally the corresponding polarization P as $P(t) = \int^t J(t')dt'$.

As mentioned above, ionization creates harmonics of the pump field only in the case if the ionization takes place on the sub-cycle timescale. If the ionization event is much slower than the optical cycle (typically associated with the multiphoton ionization regime), the nonlinearity is “too slow” to create harmonics [12]. From Eq. (2) it follows that if a persistent current arises (that is, if $J(t = \infty) \neq 0$), there must be a slow component in J which rises on the time scale of the pulse duration. This leads also to the presence of a slow component of $E_f(t)$, i.e., a 0th harmonic in $E_f(\omega) = \mathcal{F}[E_f(t)]$, where $\mathcal{F}[\cdot]$ is the Fourier transform. To obtain such persistent currents, certain type of symmetry breaking is necessary: otherwise, the number of electrons going in one direction is exactly the same as the number going in the opposite direction. In the tunnel ionization regime, if the field shape is asymmetric (for example two-color pulses or single-cycle ones), the temporal asymmetry of the field waveforms leads to spatial asymmetry of the current and thus to the generation of macroscopic persistent currents as well as the generation of 0-th harmonic of the pump.

Here, as we observe in Fig. 1(c), the mechanism leading to persistent currents should be closely related to the Freeman resonances. As explained above, this current should also generate low-frequency radiation. By plotting $E_f(\omega)$ defined by Eq. (2) in Fig. 1(d) we see that indeed low-frequency components arise. Remarkably, the spectrum contains not only well defined harmonics of the pump, but also a comb of other harmonics in the broad range up to $\omega \sim 5$ fs^{-1}, which corresponds to the visible range. The comb line-to-line distance corresponds to the inverse distance in time between the ionization peaks in Fig. 1(b). The main peak coincides with the central frequency ω_0 of the exciting pulse and corresponds to the movement of free electrons. In addition, the same picture is shown in Fig. 1(d) (red line) for the intensity of 23 TW/cm^2. In this case, the Freeman resonances are not excited and the resulting radiation at low frequencies is several orders of magnitude smaller.

The figure which demonstrates the dependence of the corresponding comb on the pulse intensity is presented in Fig. 2(a,c). One can clearly see the connection between the excitation of Freeman resonances and the generation of a broadband spectrum. Both the broadband spectrum and the

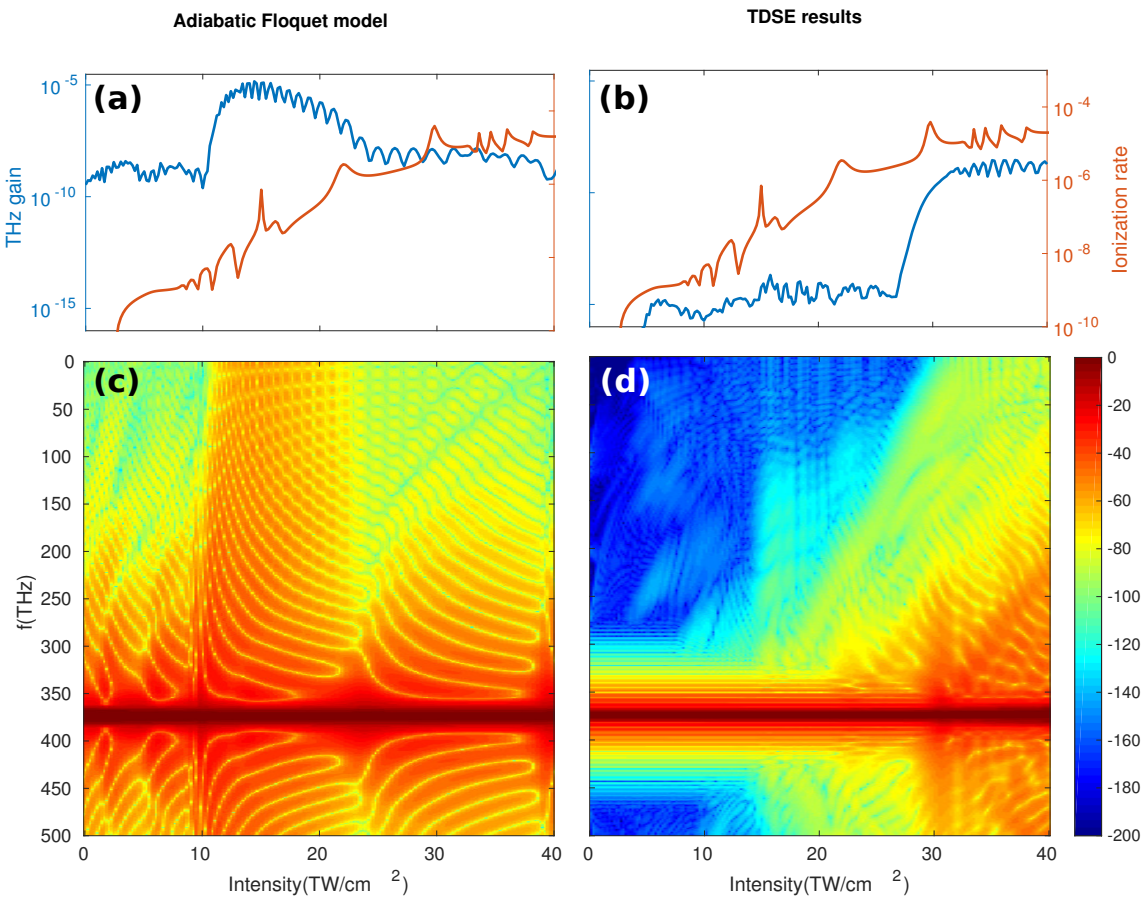

Figure 2: The generated radiation and its spectrum in dependence on the pulse intensity for the parameters of the Fig. 1, assuming the adiabatic procedure as well as the direct solution of the full Schrödinger equation. (a,b) Ionization rate according to the Floquet model (red curves) and the low frequency component of $|E_f(\omega)|^2$ (blue curves) for the case of adiabatic theory (a) and by direct solution of the Schrödinger equation (b). (c,d) Corresponding spectra in dependence of intensity for the adiabatic theory (c) and by direct solution of the Schrödinger equation (d).

presence of low frequency harmonics indicate that electron ionization dynamics contains the sub-cycle time-scale component, even though we are in the multiphoton ionization regime of the Keldysh parameter $\gamma = \omega_0\sqrt{2I_p}/E_0 \gg 1$. The Freeman resonances are so sharp, as a function of the laser intensity, that even the slowly-varying field intensity (in our adiabatic picture) passes these resonance very quickly, in less than an optical cycle. This breaks the symmetry and leads to formation of persistent currents.

Formally, as we approach the single-cycle timescale, the adiabatic approximation can no longer be used. Yet, we shall now see that the adiabatic model does offer correct qualitative insight into the exact dynamics. To this end, we now switch to the direct solution of the full time-dependent Schrödinger equation

$$i\partial_t\psi(x,t) = H\psi(x,t) \tag{3}$$

with the same Hamiltonian Eq. (1). The comparison for the pulse duration 240 fs, as a function of the pulse peak intensity, is shown in Fig. 2. The spectra generated by pulses with different intensities (and same duration) are shown both for the adiabatic approach [Fig. 2(c)] and for the exact simula-

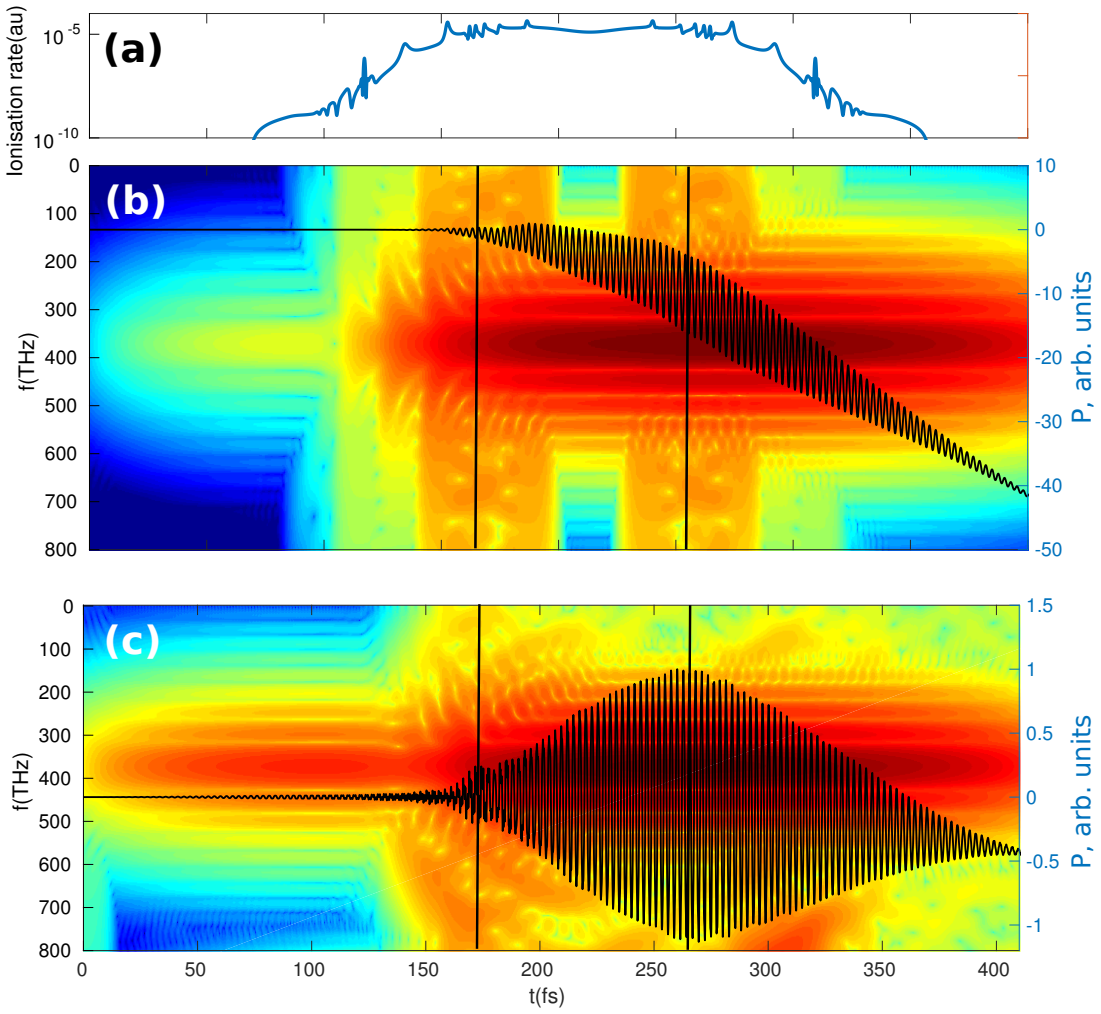

Figure 3: Comparison of the solution of full Schrödinger equation with the adiabatic procedure. (a) Ionization rate calculated using Floquet theory vs. time for a pulse with the intensity 45 TW/cm^2 and pulse duration 425.6 fs. (b,c) The XFROG diagram of the radiation $E_f(t)$ calculated according Eq. (2) (colorscale) and the corresponding dipole moment $P(t)$ (black line) according to the adiabatic theory and for TDSE calculation. Vertical black lines indicate the "center" of the first resonance and the point in time symmetric in respect to the pulse center.

tion [Fig. 2(d)]. The low-frequency part of the radiation is shown for both cases in Fig. 2(a,b) (blue lines). Red lines in Fig. 2(a,b) show the ionization rate according to the Floquet theory). One can see that, although the dynamics has some differences, it also has much in common. For instance, in the adiabatic case, the Freeman resonance at around 15 TW/cm^2 plays an obviously important role. The influence of this peak is also visible in the case of the Schrödinger equation, even though it is much less pronounced. On the other hand, the peak at around 30 TW/cm^2 plays significant role in the latter case.

In general, the figures Fig. 2(c) and Fig. 2(d) are quite different. The situation changes when we consider longer pulses. The result of more detailed comparison for longer pulses with the duration of 425.6 fs is shown in Fig. 3. We observe in Fig. 3(b,c) XFROG traces of E_f according to Eq. (2) for the adi-

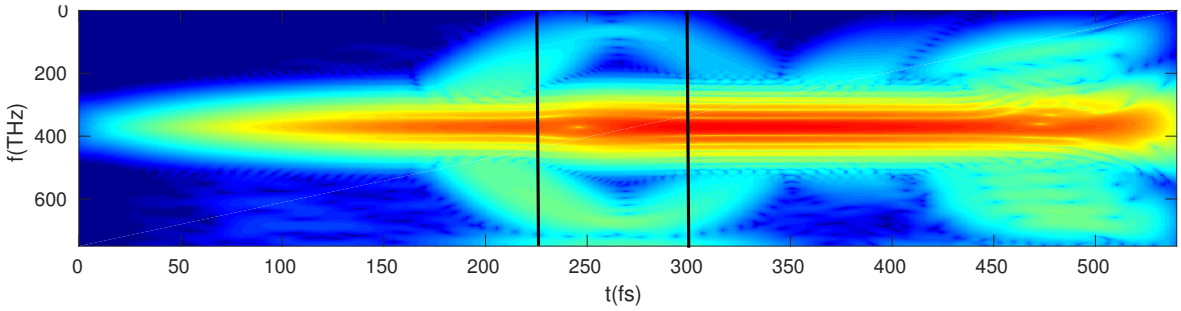

Figure 4: XFROG diagram for TDSE for 2-bound-states-atom with the potential given by Eq. (4). Black lines are put at arbitrary points symmetric in respect to the center of the exciting pulse.

abatic and TDSE approaches respectively. Fig. 3a shows the ionization rate according to the Floquet theory, while the black solid lines in Fig. 3(b,c) depict the time dependence of the polarization P. The resonances seen in the adiabatic case are now clearly visible in the TDSE calculation, showing that the agreement between the adiabatic model and the TDSE improves with increasing pulse duration.

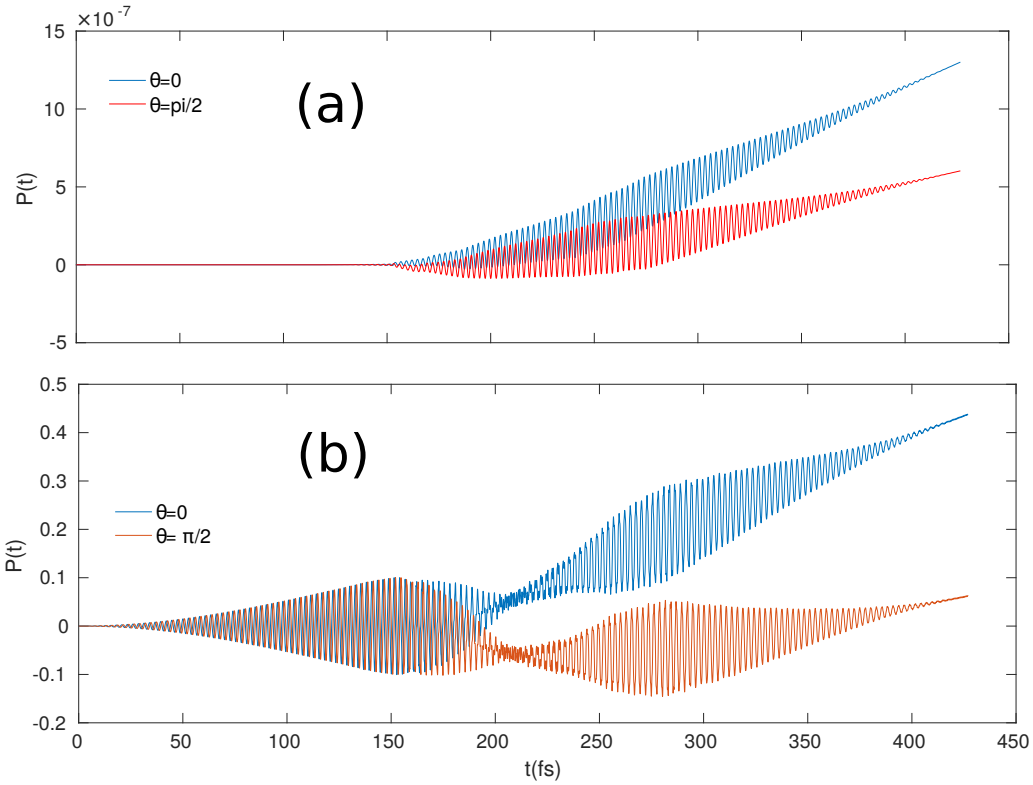

Figure 5: Dependence of the atomic polarization P on the carrier-envelope phase (CEP) in the adiabatic model (a) and for the direct solution of the time-dependent Schrödinger equation (b) for the CEP $\theta = 0$ (blue lines) and $\theta = \pi/2$ (red lines).

One important point to mention in the solution of the TDSE in Fig. 3 is the remarkable asymmetry with respect to the pulse intensity maximum (see black vertical lines in Fig. 3), indicating temporal points

symmetric with respect to the pulse maximum. This is obviously not the case for the adiabatic model. This can be explained by the fact that the first ionization event in the pulse does not only increase the number of the free electrons, but also increases population of the intermediate states of the system. The second ionization event “probes” this population. In this way, a kind of a pump-probe sequence takes place, where the role of the pump is played by the first ionization event and the role of the probe by the second ionization event. What is probed in this case is the population of highly excited bound states of the atom. To support this conclusion, we plotted in Fig. 4 the XFROG for an artificial short-range potential, which has the same ionization energy but contains only two bound states. The potential has the form:

$$V = -\frac{\exp\left(-x^{10}/\sigma^{10}\right)}{\sqrt{dx^2 + a^2}}, \tag{4}$$

with constants $\sigma = 3$, $d = 0.35$ and $a = 1.549$ (all constants in atomic units). Under these parameters, the second bound state lies around -0.2 au and close to the second bound state of the initial potential Eq. (1). One can see from Fig. 4 that the dynamics in the present case is much more symmetric (except for the feature at 450 - 500 fs, which is caused by plasma losses due to absorbing boundary). That is, we can conclude that the asymmetry of the XFROG in Fig. 3 results from the dynamics of the population trapped in high-lying bound states.

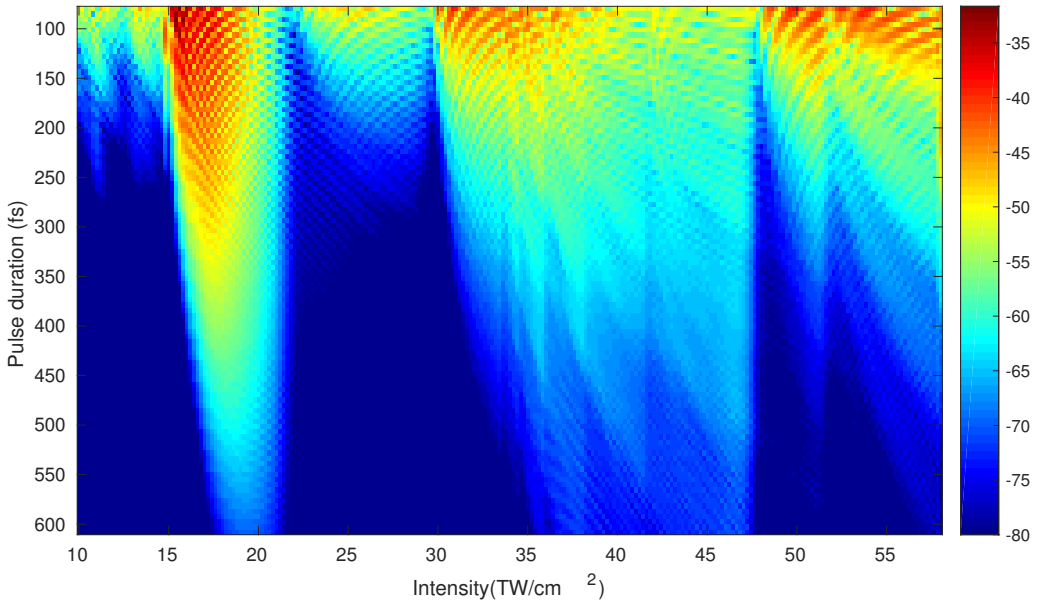

Figure 6: Dependence of the low frequency radiation component $\sim \omega^2 J(\omega)^2$ on the pulse duration and intensity (note the logarithmic scale of the colorbar).

Finally, to provide additional evidence for the sub-cycle time scale of the dynamics, we consider the dependence of the effect on the carrier envelope phase (CEP) of the pump pulse. The dynamics of the polarization P is shown in Fig. 5 for two different CEP phases, both for the adiabatic theory and for the Schrödinger equation. By observing the slope of P (since $J = \partial_t P$) one can see that the residual current is strongly CEP dependent, supporting the short-scale dynamics of the process. The same effect is visible in the Schrödinger equation simulations (Fig. 5). Thus, the effect observed here lies exactly in the transition regime between the adiabatic and non-adiabatic evolution. If we further increase the pulse duration, the slope of the intensity inside the pulse and thus the width of the resonance will also increase. As the Freeman resonance width becomes larger than the optical pulse

cycle, the transient currents and corresponding radiation should disappear. This is indeed the case, as illustrated in Fig. 6.

In conclusion, we have demonstrated that Freeman resonances lead to spatial symmetry breaking in the generation of free currents of the liberated electrons. This, in turn, leads to generation of new frequencies in a broad spectral range, similar to Brunel radiation. In particular, it provides a new source of radiation at THz frequencies and a broad comb-like spectrum from THz to the visible range. The line-to-line distance of the comb can be controlled by the pulse duration. Even more importantly, this comb-like structure as well as detailed consideration of the corresponding correlation traces show that the radiation described here contains the fingerprints of electron transition to the continuum enhanced due to the presence of intermediate resonant states, which can be used to get the information about electron dynamics in conjunction with other established approaches [27, 28, 29].

References

[1] Thomas Brabec and Ferenc Krausz. Intense few-cycle laser fields: Frontiers of nonlinear optics. *Rev. Mod. Phys.*, 72(2):545–591, Apr 2000. doi: 10.1103/RevModPhys.72.545.

[2] P. B. Corkum. Plasma perspective on strong field multiphoton ionization. *Phys. Rev. Lett.*, 71(13): 1994–1997, Sep 1993. doi: 10.1103/PhysRevLett.71.1994.

[3] Markus Kreß, Torsten Löffler, Mark D Thomson, Reinhard Dörner, Hartmut Gimpel, Karl Zrost, Thorsten Ergler, Robert Moshammer, Uwe Morgner, Joachim Ullrich, et al. Determination of the carrier-envelope phase of few-cycle laser pulses with terahertz-emission spectroscopy. *Nat. Phys.*, 2(5):327–331, 2006.

[4] Ki-Yong Kim, James H. Glownia, Antoinette J. Taylor, and George Rodriguez. Terahertz emission from ultrafast ionizing air in symmetry-broken laser fields. *Opt. Express*, 15(8):4577–4584, 2007. URL http://www.opticsexpress.org/abstract.cfm?URI=oe-15-8-4577.

[5] K. Y. Kim, A. J. Taylor, J. H. Glownia, and G. Rodriguez. Coherent control of terahertz supercontinuum generation in ultrafast laser-gas interactions. *Nat. Photon.*, 2(10):605–609, Oct 2008. ISSN 1749-4885. doi: 10.1038/nphoton.2008.153. URL http://dx.doi.org/10.1038/nphoton.2008.153.

[6] M. D. Thomson, M. Kress, T. Löffler, and H. G. Roskos. Broadband thz emission from gas plasmas induced by femtosecond optical pulses: From fundamentals to applications. *Laser & Photon. Rev.*, 1(4):349–368, 2007. ISSN 1863-8899. URL http://dx.doi.org/10.1002/lpor.200710025.

[7] Klaus Reimann. Table-top sources of ultrashort thz pulses. *Rep. Progr. Phys.*, 70(10):1597–1632, 2007. URL http://stacks.iop.org/0034-4885/70/1597.

[8] P. Sprangle, J. R. Peñano, B. Hafizi, and C. A. Kapetanakos. Ultrashort laser pulses and electromagnetic pulse generation in air and on dielectric surfaces. *Phys. Rev. E*, 69(6):066415, Jun 2004. doi: 10.1103/PhysRevE.69.066415.

[9] C. D'Amico, A. Houard, M. Franco, B. Prade, A. Mysyrowicz, A. Couairon, and V. T. Tikhonchuk. Conical forward thz emission from femtosecond-laser-beam filamentation in air. *Phys. Rev. Lett.*,

98(23):235002, 2007. doi: 10.1103/PhysRevLett.98.235002. URL http://link.aps.org/abstract/PRL/v98/e235002.

[10] I Babushkin, S Skupin, A Husakou, C Köhler, E Cabrera-Granado, L Bergé, and J Herrmann. Tailoring terahertz radiation by controlling tunnel photoionization events in gases. *New J. Phys.*, 13(12):123029, 2011. URL http://stacks.iop.org/1367-2630/13/i=12/a=123029.

[11] P González de Alaiza Martínez, I Babushkin, L Bergé, Stefan Skupin, E Cabrera-Granado, C Köhler, U Morgner, A Husakou, and J Herrmann. Boosting terahertz generation in laser-field ionized gases using a sawtooth wave shape. *Phys. Rev. Lett.*, 114(18):183901, 2015.

[12] Ihar Babushkin, Carsten Brée, Christian Markus Dietrich, Ayhan Demircan, Uwe Morgner, and Anton Husakou. Terahertz and higher-order brunel harmonics: from tunnel to multiphoton ionization regime in tailored fields. *J. Mod. Opt.*, 64(10-11):1078–1087, 2017.

[13] R. R. Freeman, P. H. Bucksbaum, H. Milchberg, S. Darack, D. Schumacher, and M. E. Geusic. Above-threshold ionization with subpicosecond laser pulses. *Phys. Rev. Lett.*, 59:1092–1095, Sep 1987. doi: 10.1103/PhysRevLett.59.1092. URL https://link.aps.org/doi/10.1103/PhysRevLett.59.1092.

[14] G. N. Gibson, R. R. Freeman, and T. J. McIlrath. Verification of the dominant role of resonant enhancement in short-pulse multiphoton ionization. *Phys. Rev. Lett.*, 69:1904–1907, Sep 1992. doi: 10.1103/PhysRevLett.69.1904. URL https://link.aps.org/doi/10.1103/PhysRevLett.69.1904.

[15] M Pont and M Gavrila. Stabilization of atomic hydrogen in superintense, high-frequency laser fields of circular polarization. *Phys. Rev. Lett.*, 65(19):2362, 1990.

[16] JH Eberly and KC Kulander. Atomic stabilization by super-intense lasers. *Science*, 262(5137):1229–1233, 1993.

[17] Maria Richter, Serguei Patchkovskii, Felipe Morales, Olga Smirnova, and Misha Ivanov. The role of the Kramers–Henneberger atom in the higher-order Kerr effect. *New J. Phys.*, 15(8):083012, 2013.

[18] H Zimmermann, S Patchkovskii, M Ivanov, and U Eichmann. Unified time and frequency picture of ultrafast atomic excitation in strong laser fields. *Phys. Rev. Lett.*, 118(1):013003, 2017.

[19] T Nubbemeyer, K Gorling, A Saenz, U Eichmann, and W Sandner. Strong-field tunneling without ionization. *Phys. Rev. Lett.*, 101(23):233001, 2008.

[20] Shih-I Chu. *Generalized Floquet Theoretical Approaches to Intense-Field Multiphoton and Nonlinear Optical Processes*, pages 739–799. John Wiley & Sons, Inc., 2007. ISBN 9780470141229. doi: 10.1002/9780470141229.ch17. URL http://dx.doi.org/10.1002/9780470141229.ch17.

[21] Michael Hofmann and Carsten Brée. Adiabatic Floquet model for the optical response in femtosecond filaments. *J. Phys. B: Atom., Molecul. Opt. Phys.*, 49(20):205004, 2016.

[22] RM Potvliege and Robin Shakeshaft. Multiphoton processes in an intense laser field: Harmonic generation and total ionization rates for atomic hydrogen. *Phys. Rev. A*, 40(6):3061, 1989.

[23] M. Born and V. Fock. Beweis des Adiabatensatzes. *Zeitschrift für Physik*, 51(3):165–180, Mar 1928. ISSN 0044-3328. doi: 10.1007/BF01343193. URL http://dx.doi.org/10.1007/BF01343193.

[24] F. Brunel. Harmonic generation due to plasma effects in a gas undergoing multiphoton ionization in the high-intensity limit. *J. Opt. Soc. Am. B*, 7(4):521–526, 1990. URL http://josab.osa.org/abstract.cfm?URI=josab-7-4-521.

[25] Byunghoon Kim, Jungkwen An, Yongli Yu, Ya Cheng, Zhizhan Xu, and Dong Eon Kim. Optimization of multi-cycle two-color laser fields for the generation of an isolated attosecond pulse. *Opt. Express*, 16(14):10331–10340, 2008. URL http://www.opticsexpress.org/abstract.cfm?URI=oe-16-14-10331.

[26] T Balciunas, AJ Verhoef, AV Mitrofanov, G Fan, EE Serebryannikov, MY Ivanov, AM Zheltikov, and A Baltuska. Optical and thz signatures of sub-cycle tunneling dynamics. *Chem. Phys.*, 414: 92–99, 2013.

[27] M. Drescher, M. Hentschel, R. Kienberger, M. Uiberacker, V. Yakovlev, A. Scrinzi, Th Westerwalbesloh, U. Kleineberg, U. Heinzmann, and F. Krausz. Time-resolved atomic inner-shell spectroscopy. *Nature*, 419(6909):803–807, Oct 2002. ISSN 0028-0836. doi: 10.1038/nature01143. URL http://dx.doi.org/10.1038/nature01143.

[28] M. Uiberacker, Th. Uphues, M. Schultze, A. J. Verhoef, V. Yakovlev, M. F. Kling, J. Rauschenberger, N. M. Kabachnik, H. Schroder, M. Lezius, K. L. Kompa, H. G. Muller, M. J. J. Vrakking, S. Hendel, U. Kleineberg, U. Heinzmann, M. Drescher, and F. Krausz. Attosecond real-time observation of electron tunnelling in atoms. *Nature*, 446(7136):627–632, Apr 2007. ISSN 0028-0836. doi: 10.1038/nature05648. URL http://dx.doi.org/10.1038/nature05648.

[29] Aleksei M. Zheltikov, Aleksandr A. Voronin, Markus Kitzler, Andrius Baltuška, and Misha Ivanov. Optical detection of interfering pathways in subfemtosecond multielectron dynamics. *Phys. Rev. Lett.*, 103(3):033901, Jul 2009. doi: 10.1103/PhysRevLett.103.033901.